LBL-20566
Preprint

Lawrence Berkeley Laboratory
UNIVERSITY OF CALIFORNIA

Materials & Molecular Research Division

Submitted to Chemical Physics Letters

MOLECULAR BEAM PHOTOELECTRON SPECTROSCOPY OF $Ni(CO)_4$

J.E. Reutt, L.S. Wang,
Y.T. Lee, and D.A. Shirley

January 1986

Prepared for the U.S. Department of Energy under Contract DE-AC03-76SF00098

DISCLAIMER

LBL-20566

Molecular Beam Photoelectron Spectroscopy of $Ni(CO)_4$

J.E. Reutt, L.S. Wang, Y.T. Lee, and D.A. Shirley

Materials and Molecular Research Division

Lawrence Berkeley Laboratory

and

Department of Chemistry

University of California

Berkeley, California 94720

Abstract

The nickel carbonyl HeI((21.2175 eV) photoelectron spectrum has been reinvestigated with improved resolution and molecular beam sampling. The $9T_2$ and 2E photoelectron bands are shown to be intrinsically diffuse, which is attributed to D_{2d} geometries. The ordering of the next seven outer valence electronic states is proposed from a linear-least squares fit of the spectrum.

1. Introduction

Transition metal carbonyls are among the most photochemically active transition metal complexes known. It is widely accepted that the bonding of these systems is described by a synergic combination of ligand-to-metal σ bonding and metal-to-ligand π backbonding [1]. The relative importance of the σ and π bonding, however, is not firmly established.

Various theoretical and experimental studies have attempted to assess the nature of the transition metal-carbonyl bond. The molecular orbital calculations have generally upheld the metal-to-ligand π bonding contribution, but have not agreed upon its relative magnitude [2-5]. The principal experimental evidence for π-backbonding has been derived from the vibrational spectroscopy [6] and bond length determinations [7] of the neutral transition metal carbonyls. Because the bonding interaction is synergic, however, a clear distinction between σ and π contributions has not been made.

Molecular photoelectron spectroscopy is a powerful method for testing bonding contributions from individual molecular orbitals. Emission of an electron from an occupied molecular orbital is accompanied by a change in geometry and force constants for the resulting ion, indicative of the bonding nature of the molecular orbital. These changes may be evaluated from the photoelectron band. Recently Hubbard and Lichtenberger have obtained high resolution photoelectron spectra of the chromium, molybdenum, and tungsten hexacarbonyls [8]. A vibrational analysis of the T_{2g} photoelectron bands, enhanced by derivative, residual, and Fourier methods of data

analysis, revealed significant π-backbonding contributions in these systems.

The transition metal carbonyls possess very soft (80-100 cm^{-1}) bending modes which will be significantly populated in room temperature samples. All photoelectron spectroscopic investigations to date have employed thermal samples and resulted in diffuse photoelectron band shapes. Although Hubbard and Lichtenberger were able to distinguish vibrational structure, their reported vibrational features were significantly broader than their reported instrumental resolution. The question remains, therefore, whether the photoelectron bands are intrinsically diffuse, or trivially broadened by hot rotational and vibrational structure; i.e., whether the broadening is homogeneous or heterogeneous.

In this paper we report the high resolution (12 meV) HeI (21.2175 eV) photoelectron spectrum of nickel carbonyl, which has been rotationally and vibrationally cooled in a supersonic molecular beam. Despite the improved resolution and cold sample temperature, the $9T_2$ and 2E photoelectron bands, the "nickel d bands", exhibited no vibrational fine structure. The bands appear to be intrinsically diffuse, which may be explained by a strong distortion from the tetrahedral geometry of the neutral species. The next seven valence photoelectron bands originating from the loss of electrons from primarily ligand molecular orbitals are reported. Their ordering is proposed on the basis of relative intensity arguments.

2. Experimental

The molecular beam photoelectron spectrometer used in this experiment has been described in detail [9] and will be discussed only

briefly. The electron energy analyzer consisted of a double electrostatic deflector operated at a pass energy of 1.0 eV which sampled the photoelectrons at an angle of 90° with respect to the incident photon beam. The HeI (21.2175 eV) spectrum of $Ni(CO)_4$ (Pressure Chemical Co.) was recorded with multi-channel detection at a resolution of 12 meV FWHM, as measured for $^2P_{3/2}$ lines of Ar and Xe. The nickel carbonyl was diluted to a concentration of 10% in neon and expanded at a total stagnation pressure of 650 torr through a 100 μm nozzle. These experimental conditions are known to cool molecules of this size efficiently [10]. It is estimated that a rotational temperature of approximately 20°K is achieved, along with a vibrational temperature sufficiently low such that less than 2% of the molecules remain vibrationally populated.

To improve statistics and allow for a frequent recalibration of the energy scale with argon and xenon, the photoelectron spectrum was obtained as a series of short 1.5 hour scans, which were subsequently combined. The reported $9T_2$ and 2E photoelectron bands represent a summation of 21 spectra, recorded sequentially. The photoelectron bands primarily associated with the ligand orbitals were obtained by a summation of seven separate scans. These conditions permit an accuracy of ±5 meV in the measurement of absolute ionization potentials. Peak splittings reduce systematic error and may be reported with higher accuracy.

3. Results and Discussion

The valence molecular orbitals of nickel carbonyl accessible with 21.2175 eV radiation are shown schematically in Fig. 1.

3.1. $9T_2$ and 2E States ("d" bands)

The $9t_2$ and 2e molecular orbitals originate from a splitting of the five degenerate d orbitals under the tetrahedral field. Evidence for π-backbonding through the transition metal d orbitals, therefore, should be sought in the $9T_2$ and 2E photoelectron bands, which are presented in Fig. 2. A reduction in the ν_2 (primarily Ni-C symmetric stretch) frequency from the 0.047 eV value for the neutral molecule would be taken as clear evidence for the π bonding character of these molecular orbitals. The photoelectron bands are very diffuse, however, and neither a second derivitive analysis nor Fourier filtering of the photoelectron bands could elucidate vibrational fine structure above the noise level. Three explanations are available for the absence of vibrational structure in the photoelectron bands of rotationally and vibrationally cold nickel carbonyl:

(i) Direct dissociation accompanies the loss of the photoelectron, resulting in featureless bands.

(ii) Ultra-fast relaxation processes broaden individual spectral features, resulting in a diffuse spectrum.

(iii) A dramatic change in the equilibrium geometry of the molecular ion from that of the neutral molecule results in a dense and unresolvable vibrational manifold.

The onset for the first dissociative ionization process :

$$Ni(CO)_4 + h\nu \rightarrow Ni(CO)_3^+ + CO + e^-$$

occurs at 8.77(2) eV [11], 0.75(3) eV above the $9T_2$ adiabatic ionization potential. Thus direct dissociation cannot explain the absence of vibrational structure. Since internally excited species are generally associated with ultra-fast relaxation processes, relaxation is an unlikely explanation for the diffuse threshold region. We turn, therefore, to the vibrational manifolds, as determined by the vibrational selection rules governing the photoionization process for the molecular geometries involved.

A normal coordinate analysis of nickel carbonyl characterized the nine fundamental frequencies of the neutral molecule [12]. Vibrational selection rules and Franck-Condon factors limit the number of vibrational levels which will be observed in the photoelectron spectrum. If the resulting ion is of T_d symmetry, only the ν_1 (primarily the CO symmetric stretch) and ν_2 (primarily the M-C symmetric stretch) modes will be significantly excited in the photoionization of cold molecules. These vibrational modes have frequencies (ν_1=0.264 eV and ν_2=0.047 eV for the neutral [13]) that would be easily resolved by our photoelectron spectrometer. The additional complication of spin-orbit splitting of the d bands ($\lambda \approx 0.080$ eV [14]) will double these levels, but this alone will not prevent a vibrational analysis. The diffuse photoelectron bands indicate population of additional vibrational modes of the photoion, resulting from a strong distortion from a tetrahedral geometry. Both the $9T_2$ and 2E electronic states of $Ni(CO)_4^+$ are degenerate and unstable in a T_d configuaration with respect to vibrations of species e [15]. A lowering of T_d symmetry to a D_{2d} symmetry for the molecular ion would be accompanied by strong excitations of the ν_4 mode (e symmetry), which is a C-Ni-C bending

motion. This frequency is only 79 cm^{-1} (0.0098 eV) [13] for the neutral molecule, less than the instrumental resolution for this experiment. Significant excitation of the ν_4 mode, effected by a $D_{2d} \leftarrow T_d$ change in equilibrium geometry upon photoionization, is needed to explain the diffuse $9T_2$ and 2E photoelectron bands.

Minimum-internal-energy geometries for an $M(CO)_4$ species with d^9 and d^{10} electron configurations have been determined by EHMO [16-17] and LCAO-MO [18] calculations. The calculations agree on a T_d geometry for a d^{10} species, as in the case of $Ni(CO)_4$. For a d^9 system, as in the case of the $9T_2$ state of $Ni(CO)_4^+$, references [16] and [18] agree on a D_{2d} equilibrium structure, while reference [17] finds D_{2d} and C_{3v} structures to be minimum and energetically equivalent. The change in energy of the predominantly metal d orbitals with respect to geometry (Walsh diagrams) indicates that a distortion from T_d symmetry will also occur for the 2E state of $Ni(CO)_4^+$. Detailed minimum internal energy calculations have not been reported for the 2E state, however.

The diffuse $9T_2$ and 2E photoelectron bands are interpreted as manifestations of a strong distortion from T_d symmetry. The experimental and theoretical evidence support a D_{2d} structure for these states. A least-squares fit of the bands to two gaussians, representing the two electronic states, was performed to determine the distribution of internal energies of the photoions. The near 3:2 intensity ratio for the two photoelectron bands (we measure 3:2.04) closely matches the degeneracy ratio, and this had assisted in the original assignment of the photoelectron bands [19]. The similar band shapes for the two electronic states, $9T_2$ (FWHM=0.692 eV) and 2E (FWHM=0.794 eV), indicate similar bonding strengths for the molecular

orbitals. The band widths denote population of higher frequency vibrations, in addition to the ν_4 levels, and support the π-backbonding character of these molecular orbitals.

3.2. $1T_1$, T_2, $7T_2$, $1E$, $8A_1$, $6T_2$, $7A_1$ States ("CO" bands)

The seven electronic states derived from emission from orbitals of predominantly CO character comprise the photoelectron spectrum in the 13-20 eV region. This complex spectral region is presented in Fig. 3. In the earlier photoelectron spectroscopy investigation by Hillier, Guest, Higginson, and Lloyd a partial assignment of the photoelectron bands was made on the basis of ab initio SCF-MO calculations [19]. The $8T_2$, $1T_1$, $1E$, and $7T_2$ states were assigned to the 15.5 eV region and the 15.7 eV shoulder was identified as the $8A_1$ state. The higher ionization potential features in the 18-20 eV range were assigned to the $6T_2$ and $7A_1$ states. Electron correlation and orbital relaxation introduce substantial error into the calculations, however, preventing a detailed assignment of the photoelectron bands. More recent theoretical studies employing X_α-Scattered Wave-Discrete Variational and SCF-HFS calculations have failed to agree on the relative ordering of the $8t_2$,$1t_1$, $1e$, $7t_2$, and $8a_1$ molecular orbitals [3].

In cases where the localization properties of molecular orbitals do not vary significantly, the orbital degeneracies may be related to the relative intensities of photoelectron bands and assist in spectral assignments [20]. Angular distribution effects may introduce an error of up to 25% in the relative intensity versus degeneracy relationship. A linear least squares fit of the photoelectron spectrum in the 13-20 eV region was performed with seven gaussian functions representing the seven electronic states. More accurate vertical ionization potentials

have been obtained by this method and the relative intensities are most consistent with an electronic state ordering of $1T_1(1\pi)$, $8T_2(5\sigma)$, $7T_2(1\pi)$, $1E(1\pi)$, $8A_1(5\sigma)$, $6T_2(4\sigma)$, and $7A_1(4\sigma)$. These results are summarized in table I and compared with theoretical calculations. The electronic states produced by the emission of 1π-derived molecular orbitals are seen to overlap and alternate in energy with the electronic states of primarily 5σ origin. Although the SCF-DV-X_α calculations offer the best agreement with observed ionization potentials, the ordering of electronic states determined from the SCFS calculations is most consistent with the present assignment of electronic states. More accurate calculations including configuration interaction are necessary to account for the severe electron correlation and orbital relaxation effects and provide a reasonable theoreticcl comparison for the experimentally observed sequence.

Acknowledgements

This work was supported by the Director, Office of Energy Research, Office of Basic Energy Sciences, Chemical Sciences Division of the U.S. Department of Energy under Contract No. DE-AC03-76SF00098.

References

[1] Mark Wrighton, Chem. Rev. 74(4) (1974) 401.

[2] E.J. Baerends and P. Ross, Mol. Phys. 30(6) (1975) 1735.

[3] Bong-Il Kim, Hirohiko Adachi, and Shosuke Imoto, J. Elec. Spec. and Rel. Phen. 11 (1977) 349.

[4] I.H. Hillier and V.R. Sanders, Mol. Phys. 22 (1971) 1025.

[5] K.H. Johnson and U. Wahlgren, Int. J. Quant. Chem. 6 (1972) 243.

[6] L.H. Jones, R.S. McDowell, and M. Goldblatt, J. Chem. Phys. 48 (1968) 2663; Inorg. Chem. 8 (1969) 2349.

[7] F.A. Cotton and R.M. Wing, Inorg. Chem. 4 (1965) 314,

[8] John L. Hubbard and Dennis L. Lichtenberger, J. Amer. Chem. Soc. 104 (1982) 2132.

[9] J.E. Pollard, D.J. Trevor, Y.T. Lee, and D.A. Shirley, Rev. Sci. Inst. 52 (1981) 1837.

[10] A. Amirov, U. Even, J. Jortner, Chem. Phys. 51 (1980)31.

[11] G. Distefano, J. Res. of the Nat. Bur. Std. A 74A (1970) 233.

[12] Hiromu Murata and Kiyoyasu Kawai, J. Chem. Phys. 26 (1957) 1355.

[13] Llewellyn H. Jones, J. Chem. Phys. 28(6) (1958) 1215.

[14] J. S. Griffith, The Theory of Transition Metal Ions (Cambridge University Press, London, 1971).

[15] Gerhard Herzberg, Molecular Spectra and Molecular Structure, Vol. III (Van Nostrand Reinhold Co., New York, 1966).

[16] Mihai Elian and Roald Hoffman, Inorg. Chem. 14(5) (1975) 1058.

[17] David A. Pensak and Ronald J. McKinney, Inorg. Chem. 18(12) (1979) 3407.

[18] Jeremy K. Burdett, J. Chem. Soc. Faraday Trans. 2(70) (1974) 1599.

[19] I.H. Hillier, M.F.Guest, B.R. Higginson, and D.R. Lloyd, Mol. Phys.

27(1) (1974) 215.

[20] Alan H. Cowley, Prog. in Inorg. Chem. 26 (1979) 46.

Table 1.
Experimental and calculated assignment of $Ni(CO)_4^+$ outer valence electronic states (ev)

Electronic State	Vertical I.P. (from gaussian mean)	Band FWHM	Relative Intensity	% Error Intensity/ Degeneracy	Former Expt.[a]	Calculations		
						SCFS[b]	SCF-DV-Xα[c]	HF[d] (Koopman's)
$9T_2(3d)$	8.722(10)	0.692	0.25	2	8.9	11.7	9.3	10.8
$2E(3d)$	9.674(10)	0.794	0.17	2	9.8	13.0	10.3	7.0
$1T_1(1\pi)$	14.009(20)	0.718	0.57	15	14.1	16.7	14.1 ($8T_2$)	17.5 ($8T_2$)
$8T_2(5\sigma)$	14.740(20)	0.855	0.64	7	14.9	17.0	14.6 ($1T_1$)	17.8 ($1T_1$)
$7T_2(1\pi)$	15.351(20)	0.859	0.47	3		17.0 (1E)	15.0 ($8A_1$)	18.0 ($7T_2$)
$1E(1\pi)$	16.058(20)	0.869	0.25	22		17.0 ($7T_2$)	15.0 ($7T_2$)	18.1 (1E)
$8A_1(5\sigma)$	16.756(20)	0.880	0.23	7	15.7	17.6	15.1 (1E)	18.9
$6T_2(4\sigma)$	18.252(20)	1.580	1.00	7	18.2	19.3	16.5	21.6
$7A_1(4\sigma)$	19.599(20)	0.837	0.36	7	19.7	20.4	17.2	22.0

[a] I.H. Hillier, M.F. Guest, B.R. Higginson, and D.R. Lloyd, Mol. Phys. 27(1) (1974) 215.

[b] Bonk-Il Kim, Hirohiko Adachi, and Shosuke Imoto, J. Elec. Spec. and Rel. Phen. 11 (1977) 349.

[c] E.J. Baerends and P. Ross, Mol. Phys. 30(6) (1975) 1735.

[d] I.H. Hillier and V.R. Sanders, Mol. Phys. 22 (1971) 1025.

Figure Captions

Fig. 1. The molecular orbitals of $Ni(CO)_4$ accessible with 21.2175 eV photons are represented schematically by the splitting of the atomic nickel and molecular CO levels within the T_d field.

Fig. 2. The 21.2175 eV photoelectron spectrum of the $Ni(CO)_4$ "d" bands is plotted above with the results of a linear least-sqares fit of the bands to two gaussians. The second derivitive of the fourier-filtered spectrum is plotted below, revealing the absence of vibrationally resolved structure at this resolution (12 meV).

Fig. 3. The 21.2175 eV photoelectron spectrum of the "CO" bands is plotted together with the results of the linear least-squares fit to seven gaussians. All fitting parameters are given in Table I. The arrows denote peaks resulting from the CO impurity in the beam.

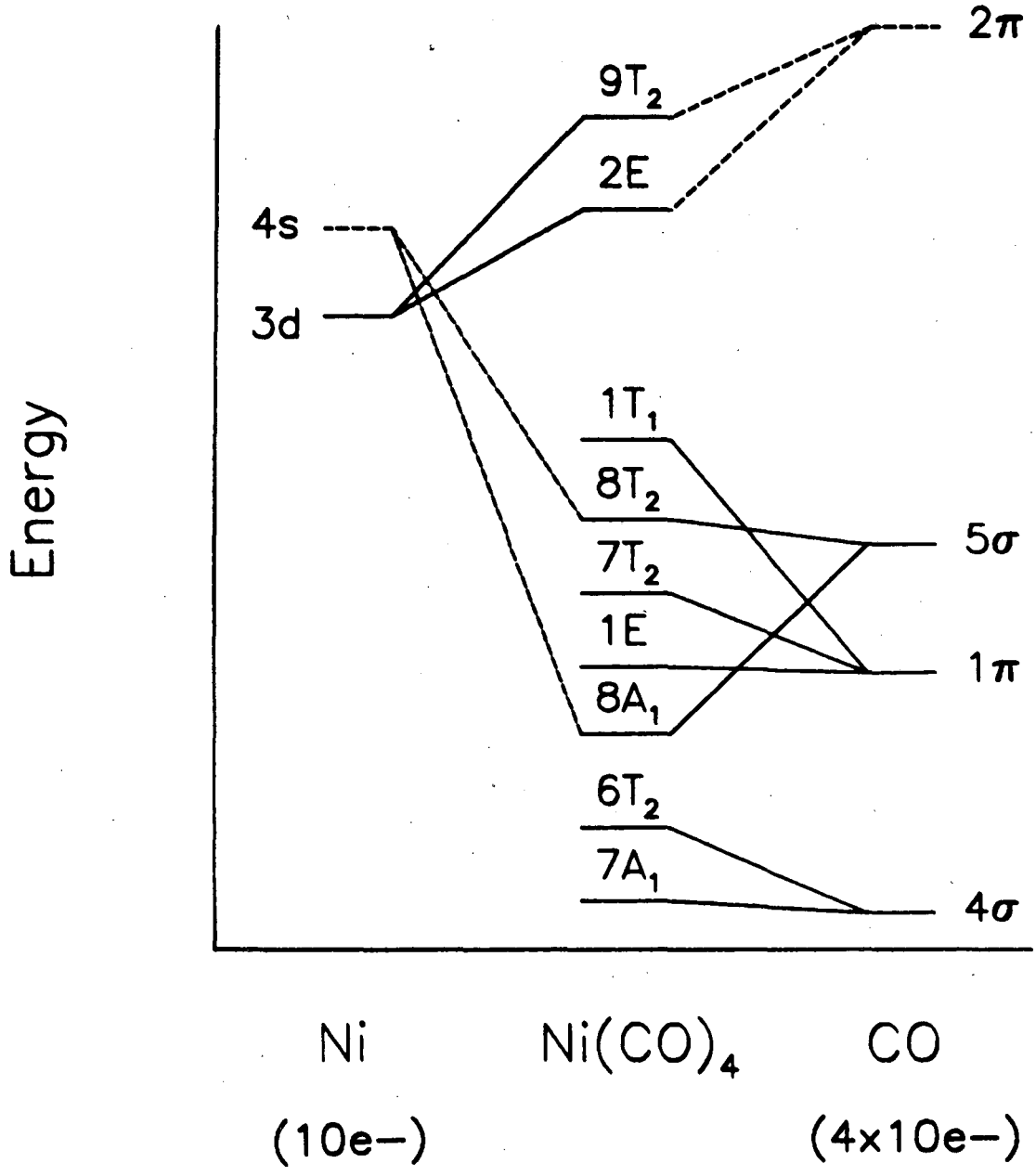
Energy
2π
9T2
2E
4s
3d
1T1
8T2
5σ
7T2
1E
1π
8A1
6T2
7A1
4σ
Ni
Ni(CO)4
CO
(10e−)
(4x10e−)
XBL 8512-5067

Figure 1

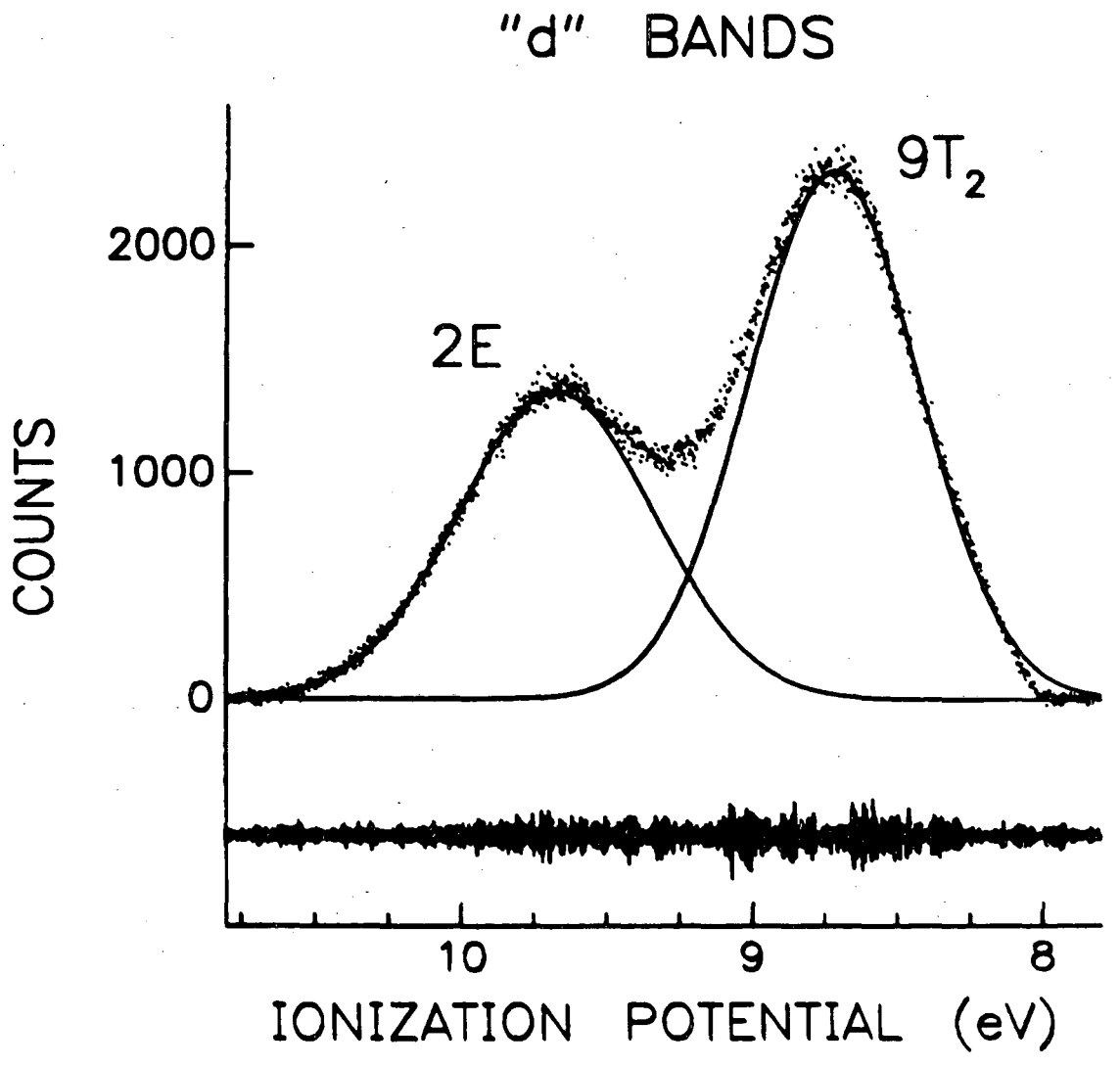

XBL 8512-5069

Figure 2.

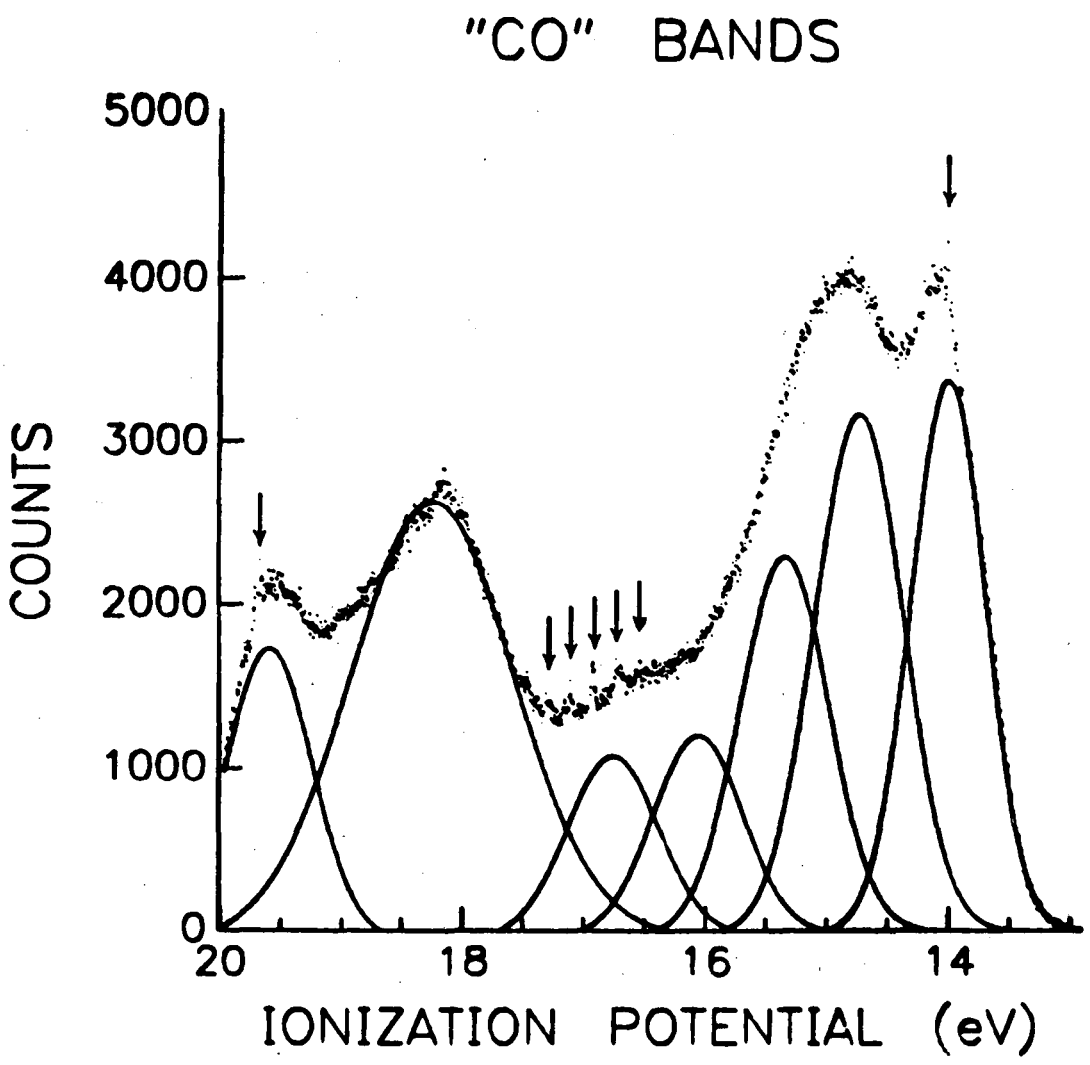

XBL 8512-5068

Figure 3

LAWRENCE BERKELEY LABORATORY
TECHNICAL INFORMATION DEPARTMENT
UNIVERSITY OF CALIFORNIA
BERKELEY, CALIFORNIA 94720